



### **Science Arts & Métiers (SAM)**

is an open access repository that collects the work of Arts et Métiers Institute of Technology researchers and makes it freely available over the web where possible.

This is an author-deposited version published in: <https://sam.ensam.eu>  
Handle ID: <http://hdl.handle.net/10985/8661>

#### **To cite this version :**

M.H. STAIA, M. SUAREZ, Didier CHICOT, J. LESAGE, Alain IOST - Cr<sub>2</sub>C<sub>3</sub>-NiCr VPS thermal spray coatings as candidate for chromium replacement - Surface and Coatings Technology - Vol. 220, p.225-231 - 2013

Any correspondence concerning this service should be sent to the repository

Administrator : [scienceouverte@ensam.eu](mailto:scienceouverte@ensam.eu)



# Cr<sub>2</sub>C<sub>3</sub>–NiCr VPS thermal spray coatings as candidate for chromium replacement

M.H. Staia <sup>a,\*</sup>, M. Suárez <sup>a</sup>, D. Chicot <sup>b</sup>, J. Lesage <sup>b</sup>, A. Iost <sup>c</sup>, E.S. Puchi-Cabrera <sup>a,b,d</sup>

<sup>a</sup> School of Metallurgical Engineering and Materials Science, Faculty of Engineering, Universidad Central de Venezuela, Apartado 49141, Caracas 1042-A, Venezuela

<sup>b</sup> Université Lille Nord de France, F-59000 Lille; USTL, LML, CNRS, UMR 8107, F-59650 Villeneuve d'Ascq, France

<sup>c</sup> Arts et Métiers ParisTech – Centre de Lille, 8, Boulevard Louis XIV, 59000 Lille Cedex, France

<sup>d</sup> Venezuelan National Academy for Engineering and Habitat, Palacio de las Academias, Postal Address 1723, Caracas 1010, Venezuela

## A B S T R A C T

The present investigation has been carried out with the aim of determining the tribological behavior of a VPS chromium carbide coating both in the as-deposited and heat-treated conditions. A commercial powder of Cr<sub>2</sub>C<sub>3</sub>–25% NiCr was sprayed employing a VPS system (Medicoat AG, Switzerland) onto plain low carbon steel coupons. The samples were subsequently annealed for 2 h at 600 °C, 800 °C and 900 °C in Ar. The microstructural characterization was carried out by using SEM and XRD before and after the heat treatment of the samples. SEM observations were employed for determining the degradation mechanisms that took place during the wear tests. When the coated systems rubbed against alumina under a 5 N normal load in air, a progressive change in the mechanism, from a mixed adhesive and abrasive, to a predominant abrasive was observed, as the heat treatment temperature increased. The wear constants were found to be of the order of approximately 10<sup>−6</sup> mm<sup>3</sup>/N.m, which indicates a wear resistance of nearly 4 times higher in comparison with the wear results reported in the literature for similar coating systems obtained by employing HVOF deposition. However, the heat treatment carried out at 900 °C brought about only 20% increase in the sliding wear resistance of the coated system.

## Keywords:

Cr<sub>2</sub>C<sub>3</sub>–NiCr coatings  
VPS deposition  
Tribological behavior  
Wear mechanisms  
Wear resistance

## 1. Introduction

A significant amount of research was carried out worldwide in the last two decades with the aim of substituting the hard chromium coatings (EHC) by using alternative and competitive processing due to the regulation concerning the emission of chromium launched in November 1994 in the United States by the Environmental Protection Agency (EPA), which put the hard chrome plating companies under pressure [1]. Both the harmful effects on Cr<sup>6+</sup> on the environment and the public health coupled with their intrinsic technical limitations such as cracks, which hinders their resistance to both alternative stresses and corrosion, are well known.

In this regard, thermal spray processes have been the leading candidates, since they produce competitive coatings from the wear and corrosion resistance point of view. A variety of industries successfully use thermally sprayed coatings and their success could be measured by their sales volume which achieved more than six billion Euros worldwide, whereby about 30% of this sum total is achieved in the European market [2]. The most common cermet coatings employed with success for substituting the hard chromium deposits were WC–Co, WC–CoCr and Cr<sub>3</sub>C<sub>2</sub>–NiCr and these have been traditionally produced by using HVOF technology [3–7].

Lately, different research results were reported for the production of cermets by plasma spraying, since it was considered to be the most flexible coating technique among thermal spray technologies [8–11].

Despite chromium carbide's excellent wear- and corrosion-resistant properties, it is not used as primary carbide in industry owing to its lower hardness in comparison to other carbides (such as tungsten carbide). Therefore, several attempts have been made to improve the hardness, wear property and corrosion of chromium carbide coatings by varying the coating techniques, processing parameters, characteristics of the feedstock powder [12–16] and the post heat treatments [17–22].

The present research is carried out with the aim of determining the tribological behavior of VPS chromium carbide in both as-deposited and heat-treated conditions. The targeted applications are related to chemical, paper and printing and mechanical industries. The results will be compared with those published in the literature that correspond to the same type of coating, but produced by using the HVOF traditional method of deposition.

## 2. Experimental

Parallelepiped samples of 20 × 20 × 4 mm<sup>3</sup> were machined and subsequently degreased with acetone. Prior to the deposition process, the samples were grid blasted with Al<sub>2</sub>O<sub>3</sub> (grade 24), which led to an average surface roughness of 5 μm. A commercial powder of Cr<sub>2</sub>C<sub>3</sub>–25% NiCr was sprayed with a Medipart M50 plasma gun (equivalent to type F4) to obtain coatings of approximately 500 μm in thickness, using a vacuum

plasma system (EMPA — Switzerland) at a pressure of 60 mbars, employing a voltage of 54 V, an argon flow of 48 l.min<sup>-1</sup> and a current of 800 A. Deposition was carried out at a standoff distance of 37 cm. Coatings were then ground and polished to achieve a final thickness of approximately 450 µm. The coating porosity was determined by means of electrochemical polarization techniques, which are described elsewhere [23,24].

Part of the samples was heat-treated in Ar to prevent oxidation of the coated system. The disks were placed inside the furnace, which was evacuated of air, filled with argon and heated at 5 °C/min. The coatings were held for 2 h at 600 °C, 800 °C and 900 °C, respectively before being cooled to 400 °C at the same rate and then allowed to cool to room temperature. Vickers hardness both in the as-deposited and heat treated coatings was determined employing a load of 300 g applied for 15 s on the coating deposition plane. The reported hardness values correspond to the mean of 10 indentations.

XRD was performed using a Siemens D500 diffractometer (Cu-Kα (λ = 1.5418 Å) radiation) to determine whether the composition of chromium carbide coating was altered from the starting feed-stock powder, as well as for determining the microstructural evolution of the coatings during the annealing process.

The tribological evaluation was performed on the coated samples prior and after heat treatment, following their metallographic preparation. Sliding wear tests were carried out employing a tribometer under ball-on-disk geometry, with an alumina ball (Φ = 6 mm) as counterpart, a contact radius of 8 cm and a 5 N normal load. Subsequently, the wear tracks were evaluated by means of SEM-EDS analysis and the worn volume determined by optical profilometry.

### 3. Results and discussion

#### 3.1. Microstructure and morphology

The diffraction patterns shown in Fig. 1 correspond to the starting powder, the coating in the as-deposited condition and the coatings annealed at different temperatures.

If a comparison between the peaks corresponding to the XRD patterns of the spraying powder and the coating in the as-deposited condition is conducted, the presence of two forms of orthorhombic Cr<sub>3</sub>C<sub>2</sub>, one with the space group Pnam (62) (JCPDS 03-71-2287) and the other with the space group Cmcm (63) (JCPDS 03-65-0897), were determined together with a NiCr solid solution (JCPDS 03-065-0380), Cr<sub>7</sub>C<sub>3</sub> (JCPDS 03-36-1482) and Cr<sub>23</sub>C<sub>6</sub> (JCPDS 03-85-1281). These findings corroborate those reported in the literature, indicating that during VPS deposition, part of the chromium and carbon contained in the Ni solid solution could decompose and precipitate as Cr<sub>2</sub>C<sub>3</sub>, Cr<sub>7</sub>C<sub>3</sub> and Cr<sub>23</sub>C<sub>6</sub>, a reaction that could occur immediately after the sprayed powder particles arrived on the substrate [25]. Careful examination of the XRD patterns indicates that the medium intensity peaks of Cr<sub>7</sub>C<sub>3</sub> overlap with those corresponding to the higher intensity peaks of Cr<sub>2</sub>C<sub>3</sub>. Furthermore, for example, the major intensity peak of Cr<sub>23</sub>C<sub>6</sub> for 2θ = 44.110 overlaps with the highest intensity peak of Cr<sub>7</sub>C<sub>3</sub> (2θ = 44.167). However, as pointed out by Zimmermann and Kreye [26] due to this fact, the presence of Cr<sub>7</sub>C<sub>3</sub> and/or Cr<sub>23</sub>C<sub>6</sub> in the as-sprayed coating can not be proven solely by X-ray diffraction techniques and a more sophisticated analysis such as transmission electron microscopy would be needed to clarify the microstructure [27].

Comparison between the XRD patterns corresponding to the coating in as-deposited condition with those corresponding to the heat-treated sample at different temperature indicates that no oxidation of coatings took place and some of the peaks corresponding to Cr<sub>23</sub>C<sub>6</sub> are more visible at higher annealing temperature, as expected.

A shift in the peak near the diffraction angle of 2θ = 44° approximately, along with the peak broadening was observed in the XRD spectrum for the as-deposited coating as compared to that of the starting powder, indicating the existence of an amorphous phase produced as a consequence of the massive dissolution of carbides during the deposition process, which saturates the NiCr solid solution with C and Cr. It is evident from the XRD spectra of the heat-treated coatings that microstructural transformations occurred during the thermal exposure. The increase in temperature brings about a recrystallization process, which takes place with the formation of new carbides and

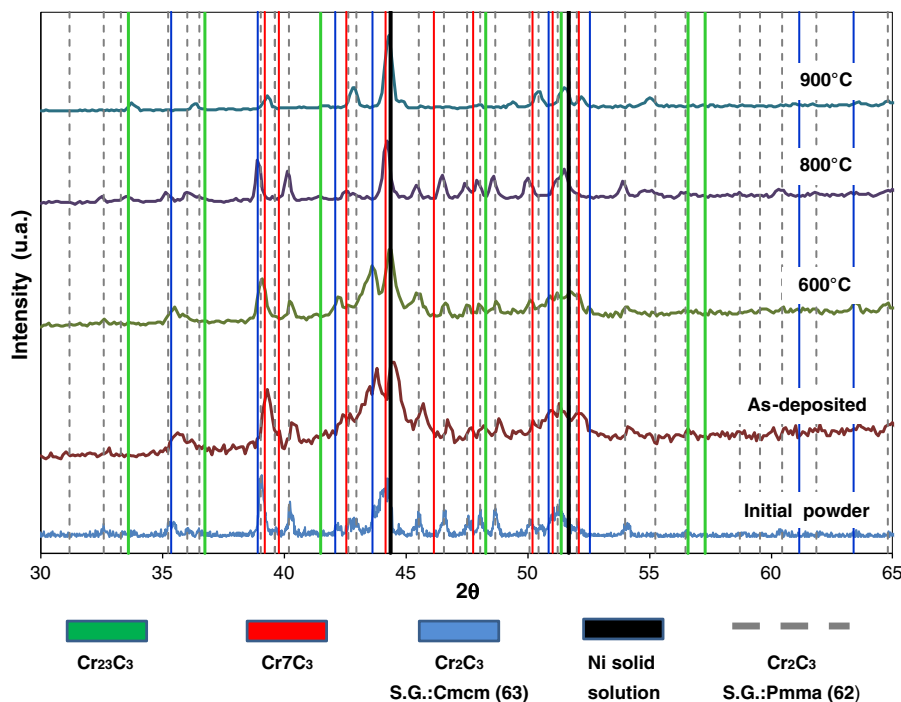


Fig. 1. XRD patterns of all the coatings under study and that corresponding to the spraying powder. The Powder Diffraction File Cards, Joint Committee on Powder Diffraction Standards, Swarthmore, PA, 1990 (now International Centre for Data (ICDD), Newtown Square, PA).

their subsequent growth, giving rise to the presence of well-defined peaks and of a higher intensity.

Fig. 2 illustrates the microstructural evolution of the coatings with the heat-treatment temperature. As can be observed from the micrograph of the coating in as-deposited condition, the large variation in the gray scale is due to the change in matrix composition as a consequence of the dissolution of carbides in the NiCr matrix during the VPS processing. The very dark isolated regions correspond to  $\text{Cr}_3\text{C}_2$  grains. Higher carbide particles, with typical angular shape, are found in the middle of the biggest splats, a morphology that has been previously reported for similar coating systems by different authors [17,21,22]. The results from the EDS analysis carried out within the regions indicated on each micrograph are reported in Table 1.

Despite that the coating porosity is of ~1–2%, in Fig. 2b it can be noticed the presence of small cracks between lamellas, which is probably due to the existence of residual stresses produced during deposition, whose values increase as the thickness of the coating increases [28]. As the heat-treatment temperature reached 900 °C, a substantial increase in the number of carbides takes place that leaves the matrix depleted of C and Cr. As can be observed in region “1” of the photomicrograph shown in Fig. 2d, the matrix appears as the white phase surrounding the carbides. As it could be noticed in the Ni X-ray mapping performed in the region at the interface between the coating and substrate for this temperature, most of the Ni diffuses towards the substrate ensuring the presence of a metallurgical bond, which improves the coating adhesion (see Fig. 3) and therefore, confirming the variation of the Ni concentration presented in Table 1.

### 3.2. Coatings hardness

Contradictory results have been published in the literature [29–31] regarding the effect of the heat-treatment on hardness. However, these results should be analyzed carefully, since they depend of the coating structure, heat treatment conditions such as environment and

**Table 1**

Results from the EDS analysis performed within the regions indicated in each SEM micrograph in Fig. 2.

Micrograph	Element	Region 1		Region 2		Region 3	
		wt%	at%	wt%	at%	wt%	at%
Coating As-received	C K	19.99	52.15	11.98	30.60	16.24	46.30
	CrK	74.43	44.87	44.42	26.98	64.05	42.19
	NiK	5.58	2.98	42.60	22.27	19.71	11.51
Coating Heat-treated at 600 C	C K	18.83	50.18	17.30	48.24	13.41	41.53
	CrK	78.73	48.46	62.90	40.52	44.90	32.11
	NiK	2.44	1.36	19.80	11.24	41.69	26.36
Coating Heat-treated at 800 C	C K	15.64	44.97	16.71	47.10	12.06	38.34
	CrK	71.18	47.28	65.59	42.69	60.98	44.77
	NiK	13.18	7.75	17.70	10.21	26.96	16.88
Coating Heat-treated at 900 C	C K	15.23	45.25	14.91	44.13	19.12	50.77
	CrK	40.82	28.03	55.56	37.99	75.32	46.20
	NiK	43.95	26.72	29.52	17.88	5.56	3.03

time, as well as on the indentation practice, related to indentation load and the way it is applied.

The heat treatment of the VPS  $\text{Cr}_3\text{C}_2$ –NiCr coating at 900 °C gave rise to a reduction in the hardness from  $1393 \pm 79 \text{ HV}_{300}$ , corresponding to the coating in the as-deposited condition, to  $1121 \pm 66 \text{ HV}_{300}$  (see Fig. 4), as consequence of both the recovery and recrystallization of the matrix, as well as to the coarsening of the precipitates as the annealing temperature increases. This phenomenon is probably due to a decrease in the dislocation density, which in turn produces a decrease in the material strength. It is interesting to point out that the hardness value of the as-deposited coating is slightly higher than the hardness value found in the literature for similar coated systems and for the same indentation load. This difference was explained by Tomita et al. [25], who attributed the high hardness of  $\text{Cr}_3\text{C}_2$ –Ni–Cr cermet coatings formed by VPS to the fact that these coatings have a dense lamellar structures composed of  $\text{Cr}_3\text{C}_2$ ,  $\text{Cr}_7\text{C}_3$ ,  $\text{Cr}_{26}\text{C}_3$  and NiCr solid solution,

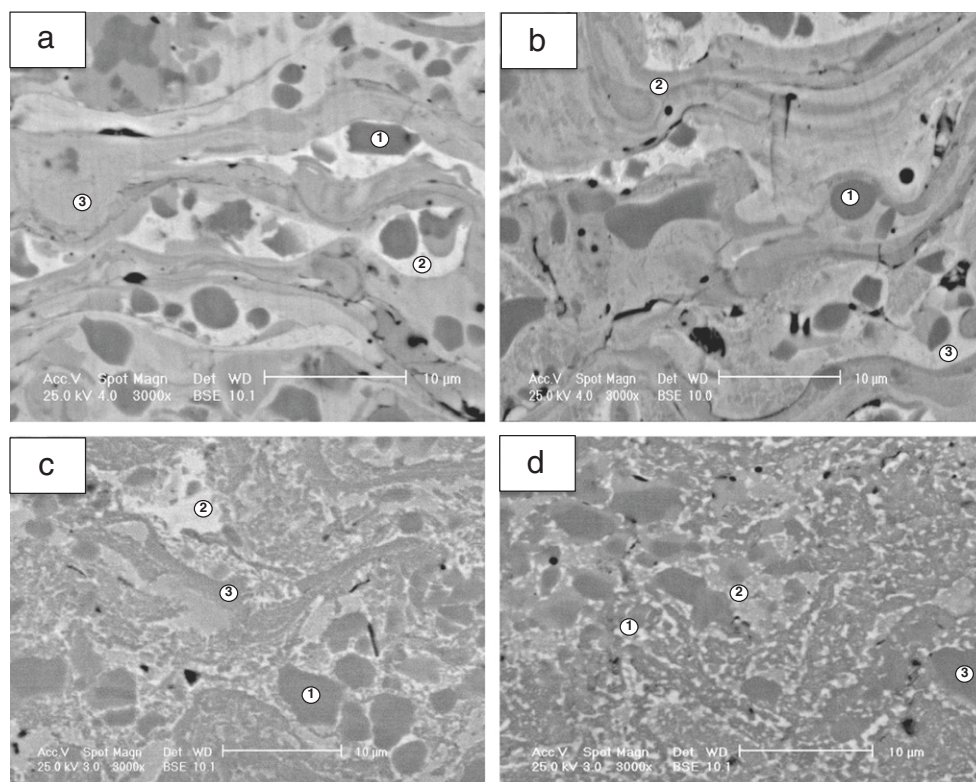


**Fig. 2.** SEM micrographs (BSE mode), indicating the microstructural evolution of the coatings with the heat treatment temperature: a. as-deposited; b. heat treated at 600 °C; c. heat treated at 800 °C; d. heat-treated at 900 °C.



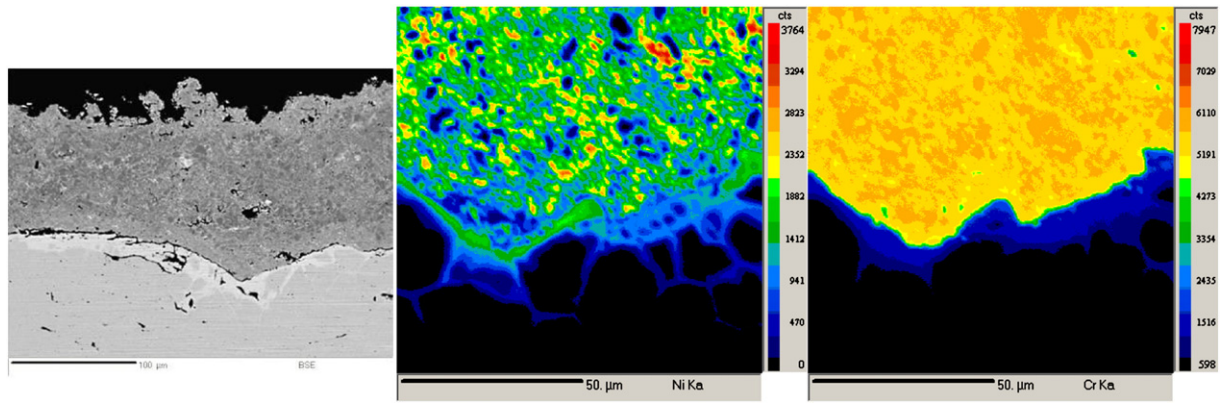


Fig. 3. X-ray mapping of the interface of the coating-substrate system heat-treated at 900 °C.

whereas HVOF coatings have also a lamellar structure, but with many fine gaps and are composed of  $\text{Cr}_3\text{C}_2$ ,  $\text{Cr}_7\text{C}_3$ ,  $\gamma\text{-NiCr}$  solid solution and a large amount of  $\text{Cr}_2\text{O}_3$ .

As it could be observed from the microstructural evolution presented in Fig. 2, for short heat-treatment times, as those used in the present investigation, the carbides will grow as independent agglomerates and, as consequence, will act as additional individual hard particles, without having a considerable influence on the global coating hardness. Similar results were reported by Matthews et al. [22], who indicated that only for long duration treatments, the increase in hardness could be significant due to carbide bonding.

### 3.3. Tribological tests

The variation of the friction coefficient values for the coated system with the sliding distance is shown in Fig. 5. The initial increase in the friction coefficient for all the tested samples could be explained in terms of the overcoming of the adhesive contact between the alumina ball and the coating. From this distance, a decrease in the friction coefficient takes place due to the strengthening of the matrix, as consequence of the applied load. As expected, this phenomenon is more pronounced for the sample heat-treated at 600 °C. After 50 m the abrasive mechanism overcomes the strengthening mechanism and the formation of debris starts to take place.

During the cyclic application of the load, debris are subjected to fatigue and, as the test continuous, they are eliminated from the contact

leaving the original surface exposed to a fresh contact with the alumina ball. Therefore, a decrease in the friction coefficient takes place, which corresponds to a change from a three-body contact back to a two-body contact mechanism. As it can be observed, for the coating in as-deposited condition, the frequency of both debris formation and elimination takes a longer time in comparison with the specimen treated at 900 °C, since the latter specimen has a higher volume fraction of precipitates, indicating that this process is highly sensitive to the microstructural characteristics of the material. The debris are continuously subjected to both fracture and chemical reaction with the environment and are eliminated from the contact. Therefore, they will have little influence on the distribution of compressive stresses during the contact with the ball. At the end of the wear tests, the amount of debris found at the wear track edge was higher for the samples heat-treated at 900 °C than for those heat-treated at 600 °C, since for the latter the adhesive wear mechanism is more pronounced bringing about a higher value of the friction coefficient between counterparts.

Fig. 6 shows the wear track of a coated sample annealed at 900 °C. The existence of cracks can be noticed, which could be attributed to both the relaxation of the tensile residual stresses existing in the original coating, as well as to the presence of the compressive stresses due to the contact with the alumina ball during the wear test.

The values of the wear constants presented in Fig. 7, calculated using Archard's law, satisfactorily describe the behavior presented in Fig. 5. It could be observed that the heat treatment brought about

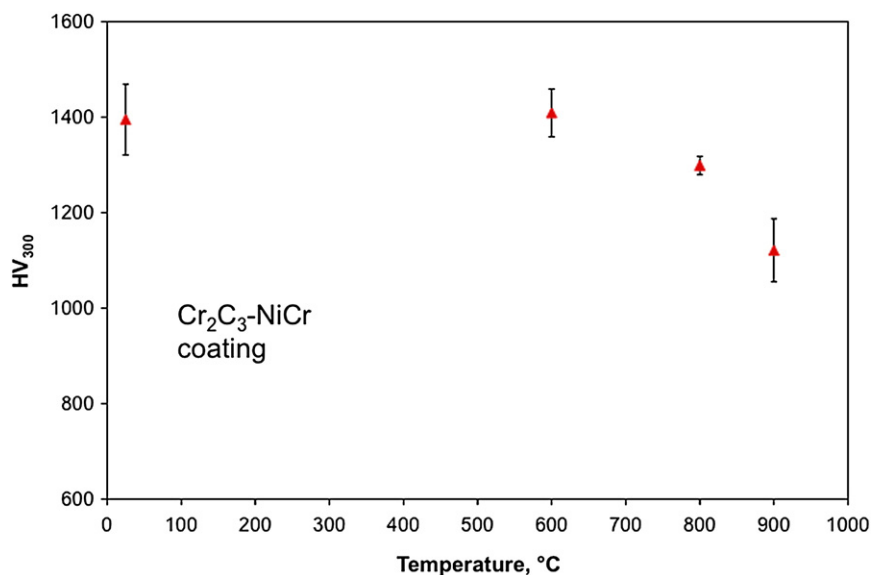
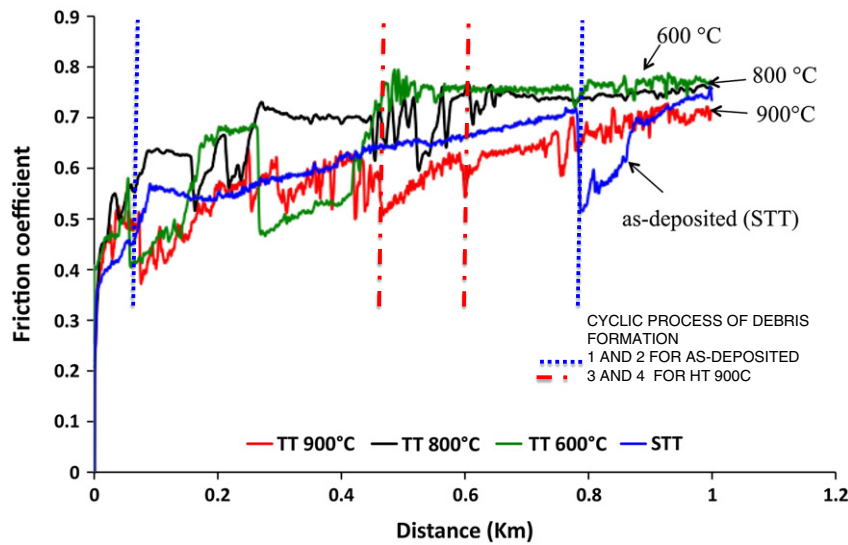


Fig. 4. Variation of the coating hardness with the heat treatment temperature.



**Fig. 5.** Evolution of the friction coefficient with the sliding distance. The dotted lines in the figure indicate the frequency of cyclic process of debris formation for the as-deposited coating and for the heat-treated coatings at 900 °C, respectively.

an increase of only ~20% in the wear resistance of the coated system in as-deposited condition, in comparison with that corresponding to the sample heat-treated at 900 °C. These results do not agree with those published by other authors [17], who claimed that microstructural changes associated with such heat-treatments could significantly improve the wear resistance of thermally sprayed cermet coatings.

However, for all the tested samples irrespective to their heat-treatment condition, wear coefficients of the order  $10^{-6}$  mm<sup>3</sup>/Nm were obtained, indicating a good wear resistance in accordance with the criteria presented by Fouroulis [32], and specially, taking into account the considerable difference in hardness between the counterparts. Nevertheless, it is thought that the slight increase in the wear resistance with the heat-treatment temperature could be attributed to the fact that the coating structure is denser and, hence, the lamellas are more constrained to undergo plastic deformation.

In the literature, several authors [10,17,33–35] have reported values for the sliding wear rates of Cr<sub>2</sub>C<sub>3</sub>–NiCr coatings from tests performed using a ball-on-disk geometry, under different test conditions such as applied normal load, velocity, nature of the counterpart as well as different post-treatments processes. This variety of conditions makes difficult a direct comparison of the values reported for the wear rate among the existing published information.

However, one way of achieving a more judicious comparison would be by taking into account the maximum Hertzian pressure

( $P_{max}$ ) during the static contact between the ball and the coated sample for equivalent test conditions. Assuming values of 124 GPa and 0.30 for the elastic modulus and Poisson's ratio of the Cr<sub>2</sub>C<sub>3</sub>–NiCr coating, 370 GPa and 0.22 for the 6 mm Al<sub>2</sub>O<sub>3</sub> ball [36,37], 640 GPa and 0.26 for the 6 mm WC–Co ball, respectively and by taking the elastic limit of NiCr–Cr<sub>2</sub>C<sub>3</sub> as 1/3 of its hardness (expressed in MPa), all the contact mechanics computations can be carried out. The results are presented in Table 2.

The equations employed for computing the values of the maximum contact pressure,  $P_{max}$ , the contact diameter,  $a$ , and the maximum Von Mises stress,  $\sigma_{max}$ , for the ball-on-disk geometry, i.e. circular contact, are described elsewhere [38]. However, in this case the composite modulus of the coated system, as a function of the contact radius, is expressed according to the formulation advanced by Döerner and Nix [39], which is subsequently employed in the computation of the reduced modulus.

The experimental results presented by Mohanty [33] and Guilemany [17], who conducted extensive sliding wear tests for the Cr<sub>2</sub>C<sub>3</sub>–NiCr HVOF coated systems under similar conditions (0.1 sliding velocity, 0.8 mm radius of the track and sliding distance of 1000 m), are also presented in order to allow their comparison with those obtained in the present study.

Mohanty et al. [33] reported a wear track cross section area of 6228 μm<sup>2</sup> for the HVOF coated system against an alumina ball of

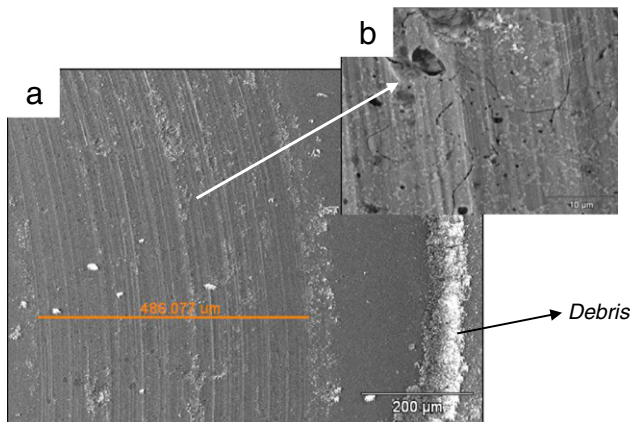


**Fig. 6.** SEM micrograph of the wear track after the sliding test for the coated sample annealed at 900 °C.

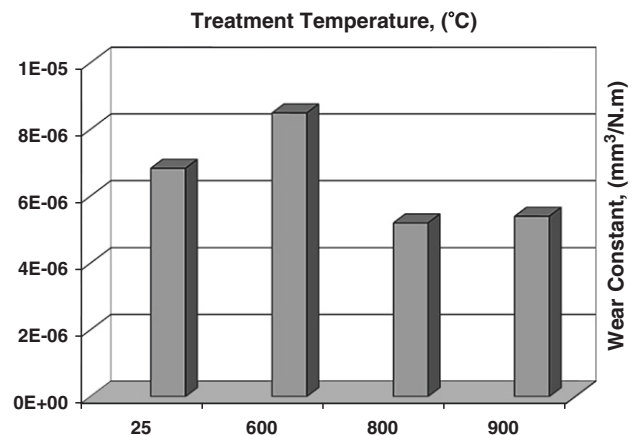


**Fig. 7.** Results from the wear tests indicating the wear constant values as function of temperature.

**Table 2**  
Results for the calculations of the maximum Hertzian pressure for the static contact.

Conditions of the wear test	a (mm)	$\sigma_{\max}$ (MPa)	$P_{\max}$ (MPa)	$A_{st}$ , cross section area of the wear scar ( $\mu\text{m}^2$ )	
VPS coating/alumina ball $\Phi = 6$ mm Load 5 N	0.048	639	1030.6	1424 (HT900°C)	Present work
HVOF coating/alumina ball $\Phi = 10$ mm Load 10 N	0.072	572	923.7	6228 (HT900 °C)	[28]
HVOF coating/WC ball $\Phi = 11$ mm Load 15 N	0.082	666	1075	3400 (HT880°C)	[17]

10 mm diameter, which slide against 0.1 m/s under a load of 10 N. This value is almost 4 times higher than the cross section area found in the present research, considering that the value of the maximum contact pressure in the former case is even less (~10%) than the maximum contact pressure applied on the VPS coating.

In case of the results obtained by Guilemany et al. [17] for a HVOF coating heat-treated at 880 °C, a volume loss of 0.017 mm<sup>3</sup> equivalent to a wear scar cross section area of 3400 mm<sup>2</sup> was determined, which is approximately 2.4 times higher than that reported in the present investigation.

The results indicated in Table 2 show that for the coating annealed at 900 °C, the maximum contact pressure was of approximately 1031 MPa and the maximum effective stress of 639 MPa. The latter is 27% higher than the value of the coating elastic limit, which was taken as 1/3 of the hardness value (in MPa), according to Tabor's rule. This last result shows that during spherical indentation with an alumina ball of 6 mm diameter under static conditions, the coating undergoes plastic deformation. Nevertheless, the stress state during the tribological tests is far more complex than the simple indentation, since there are compressive stresses in front and under the ball, as well as tension stresses behind the ball. The evolution of the von Mises stress as function of depth is presented in Fig. 8, where it can be observed that this stress value is well within the coating and that the substrate provides a good load-support.

However, the decision regarding the use of VPS coatings should be taken on the basis of a careful technical and economical analysis, since the investment costs of VPS deposition are roughly 4 times in comparison with HVOF deposition, whose process monitoring is far more easier [40].

On the other hand, it is worth mentioning that from the corrosion point of view, it has been shown [18] that during experiments using electrochemical polarization techniques, carried out on the VPS coatings heat treated at 900 °C, the corrosion current density values,  $i_{\text{corr}}$ , are nearly 4 times smaller as compared to the  $i_{\text{corr}}$  values determined for the coating in the as-received condition, as a consequence of the metallurgical bond established at the coating–substrate interface. Nevertheless, as it was indicated in a previous research [18], the fact that a high difference of the potential electrode values exists between the carbides particles and the Ni matrix, the coated system will never reach passivity in a 3.5% sodium chloride aqueous solutions, since the corrosion potential,  $E_{\text{corr}}$ , had high negative values of −419.4 mV, despite the substantial reduction of the passage of corrosive solution towards the substrate/coating interface.

On the other hand, sometimes the coating performance in service could be significantly better than at the laboratory level. For example, it was reported that High Velocity Oxy-Fuel thermal spray (HVOF) of WC–Co and WC–CoCr has been a successful alternative for hard chromium replacement, demonstrating that these coatings are far more wear and corrosion resistant in service, although their performance in the standard ASTM B117 salt fog test was inferior to EHC [3]. Therefore, as it was previously stated, there is no simple analytical tool for determining the best alternative process, since the capabilities must be matched carefully with the full range of requirements and the understanding of the systems in which these alternatives will be used.

#### 4. Conclusions

The diffraction studies carried out in the present research indicate that the spraying powder and the coatings heat-treated and in as-deposited condition contained two forms of orthorhombic Cr<sub>3</sub>C<sub>2</sub>, one with the space group Pnam (62) and the other with the space group Cmc<sub>2</sub> (63), were determined together with a NiCr solid solution, Cr<sub>7</sub>C<sub>3</sub> and C<sub>23</sub>C<sub>6</sub>. It was found that during the sliding tests, the

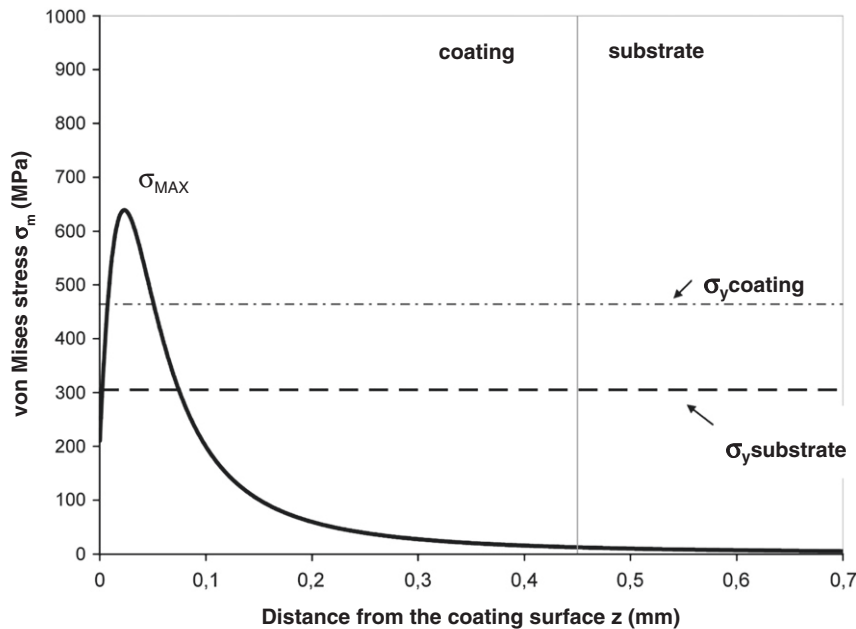


**Fig. 8.** Variation of the calculated von Mises stress as function of depth for the static contact between as-deposited sample and alumina ball.

coated systems underwent a progressive change in the mechanism, from a mixed adhesive and abrasive to a predominant abrasive, as the heat treatment temperature increases. The wear constants were found to be of the order of approximately  $10^{-6} \text{ mm}^3/\text{N.m}$ , indicating a satisfactory behavior from the tribological point of view. However, the heat treatment has no important consequences on the tribological performance of these coatings, since only a decrease of ~20% of the wear volume was determined for the heat treatment conducted at 900 °C. It was shown that the VPS method could produce a coating in as-deposited condition that is nearly 4 times more resistant to sliding wear against an alumina counterpart than those coatings obtained by HVOF deposition. However, the decision regarding the use of VPS coatings has to be taken on the basis of a careful costs–benefits analysis, since the investment costs of VPS deposition are roughly 4 times as compared to HVOF deposition, whose process monitoring is far more easier.

## Acknowledgments

The financial support of the CDCH-UCV through the Project No. PI 08-7728-2009/1 is gratefully acknowledged. EMPA-Materials Science & Technology, Switzerland, is also acknowledged for providing the samples. Professor Puchi-Cabrera acknowledges the financial support of the Conseil Régional Nord-Pas de Calais, France, through the International Chair program 2011.

## References

- [1] St. Siegmann, O. Brandt, N. Margadant, In: 1st International Thermal Spray Conference—Thermal Spray: Surface Engineering via Applied Research, Montréal, Québec, Canada, 2000, p. 1135, ISBN/ISSN: 0-87170-680-6.
- [2] G. Langer, TeroLab Surface GmbH Chairman Expert Committee 2 “Thermal coating and Autogenous Technologies” Competitive solutions for coating technology DVS—German Welding Society, Aachener Str. 172, 40223, Dusseldorf, 2010, pp. 1–15.
- [3] B. Sartwell, K. Legg, P.E. Bertz, In: Proceedings of the AESF Aerospace Plating and Metal Finishing Forum, March 2000, p. 131.
- [4] D.-Y. Kim, M.-S. Han, J.-G. Youn, In: C.C. Berndt (Ed.), Thermal Spray: Practical Solutions for Engineering Problems, ASM International, Materials Park, OH, USA, 1996, p. 123.
- [5] U. Erning, M. Nestler, In: Proceedings of United Thermal Spray Conference (UTSC 99), Düsseldorf, Marzo 1999, p. 462.
- [6] T. Sahraoui, S. Guessasma, N.E. Fenineche, G. Montavon, C. Coddet, Mater. Lett. 58 (2004) 654.
- [7] A.C. Savarimuthu, I. Megat, H.F. Taber, J.R. Shadley, E.F. Rybicki, W.A. Emery, J.D. Nuse, D.A. Somerville, In: Proceedings of 1st International Thermal Spray Conference (ITSC 2000), Canada, 2000, p. 1095.
- [8] P. Fauchais, G. Montavon, M. Vardelle, J. Cedelle, Surf. Coat. Technol. 201 (2006) 1908.
- [9] Y.C. Zhu, K. Yukimura, C.X. Ding, P. Yu Zhang, Thin Solid Films 388 (2001) 277.
- [10] M.H. Staia, T. Valente, C. Bartuli, D.B. Lewis, C.P. Constable, Surf. Coat. Technol. 146–147 (2001) 553.
- [11] J.M. Guilemany, S. Dosta, J.R. Miguel, Surf. Coat. Technol. 201 (2006) 1180.
- [12] V. Singh, R. Diaz, K. Balani, A. Agarwal, S. Seal, Acta Mater. 57 (2009) 335.
- [13] J. Wang, B. Sun, Q. Guo, M. Nishio, H. Ogawa, J. Therm. Spray Technol. 11 (2002) 261.
- [14] J.K.N. Murthy, B. Venkataraman, Surf. Coat. Technol. 200 (2006) 2642.
- [15] D.E. Wolfe, T.J. Eden, J.K. Potter, A.P. Jaroh, J. Therm. Spray Technol. 15 (2006) 400.
- [16] M. Factor, I. Roman, J. Therm. Spray Technol. 11 (2002) 468.
- [17] J.M. Guilemany, J.M. Miguel, S. Vizcaino, C. Lorenzana, J. Delgado, J. Sanchez, Surf. Coat. Technol. 157 (2002) 207.
- [18] M. Suarez, S. Bellayer, M. Traisnel, W. Gonzalez, D. Chicot, J. Lesage, E.S. Puchi-Cabrera, M.H. Staia, Surf. Coat. Technol. 202 (2008) 4566.
- [19] S. Wirojanupatump, P.H. Shipway, D.G. McCartney, Wear 249 (2001) 829.
- [20] V. Stoica, R. Ahmed, T. Itsukaichi, Surf. Coat. Technol. 199 (2005) 7.
- [21] K. Tao, X. Zhou, H. Cui, J. Zhang, Surf. Coat. Technol. 203 (2009) 1406.
- [22] S. Matthews, M. Hyland, B. James, Acta Mater. 51 (2003) 4267.
- [23] M. Urgan, A.F. Çakir, O.L. Eryilmaz, C. Mitterer, Surf. Coat. Technol. 71 (1995) 60.
- [24] E. Celik, I. Ozdemir, E. Avci, Y. Tsunekaw, Surf. Coat. Technol. 193 (2005) 297.
- [25] T. Tomita, Y. Takatani, K. Tani, Y. Harada, In: C.C. Berndt, K.A. Khor, E.F. Lugscheider (Eds.), Thermal Spray 2001: New Surfaces for the New Milenium, Proceedings of the International Thermal Spray Conference, ASM International, Materials Park, Ohio, USA, 2001, p. 699.
- [26] S. Zimmermann, H. Kreye, In: C.C. Berndt (Ed.), Thermal Spray: Practical Solutions for Engineering Problems, ASM International, Materials Park, Ohio, USA, 1996, p. 147.
- [27] G.-C. Ji, C.-J. Li, Y.-Y. Wang, W.-Y. Li, Surf. Coat. Technol. 200 (2006) 6749.
- [28] T.W. Klyne, S.C. Gill, J. Therm. Spray Technol. 5 (4) (1996) 401.
- [29] J. He, E.J. Lavernia, Mater. Sci. Eng., A 301 (2001) 69.
- [30] Y. Fukuda, M. Kumon, In: A. Ohmori (Ed.), Thermal Spraying: Current Status and Future Trends, High Temperature Society of Japan, 1995, p. 107.
- [31] F. Otsubo, H. Era, T. Uchida, K. Kishitake, J. Therm. Spray Technol. 9 (4) (2000) 499.
- [32] Z.A. Foroulis, Wear 96 (1984) 203.
- [33] M. Mohanty, R.W. Smith, M. De Bonte, J.P. Celis, E. Lugscheider, Wear 198 (1996) 251.
- [34] J.A. Picas, A. Forn, A. Igartua, G. Mendoza, Surf. Coat. Technol. 174–175 (2003) 1095.
- [35] L. Fedrizzi, S. Rossi, R. Cristel, P.L. Bonora, Electrochim. Acta 49 (2004) 2803.
- [36] J. Li, C. Ding, Surf. Coat. Technol. 135 (2001) 229.
- [37] In: M. Baucio (Ed.), ASM Engineered Materials Reference Book, Second edition, ASM International, Materials Park, OH, 1994.
- [38] K.L. Johnson, Contact Mechanics, Cambridge University Press, 1985.
- [39] M.F. Doerner, W.D. Nix, J. Mater. Res. 1 (1986) 601.
- [40] T.S. Sidhu, R.D. Agrawal, S. Prakash, Surf. Coat. Technol. 198 (2005) 441.